ELSEVIER

Carbohydrate Research 265 (1994) 97–111

CARBOHYDRATE RESEARCH

Molecular recognition of antigenic polysaccharides: a conformational comparison of capsules from *Streptococcus pneumoniæ* serogroup 9

Trevor J. Rutherford [a,1], Christopher Jones [a,*], David B. Davies [b], A. Clare Elliott [c]

[a] *Laboratory for Molecular Structure, National Institute for Biological Standards and Control, Blanche Lane, South Mimms, Potters Bar, Hertfordshire EN6 3QG, United Kingdom*

[b] *Chemistry Department, Birkbeck College, University of London, Gordon House, 29 Gordon Square, London WC1H OPP, United Kingdom*

[c] *ZENECA Agrochemicals, Jealott's Hill Research Station, Bracknell, Berkshire RG12 6EY, United Kingdom*

Received 21 March 1994; accepted 11 June 1994

Abstract

Aqueous solution conformations of three antigenic bacterial capsular polysaccharides (CPS) from *S. pneumoniæ* serogroup 9 were determined using a combination of NMR data (NOE build-up rates and conformation-dependent chemical shifts), simulated annealing, and molecular dynamics simulations. Each polymer adopts a flexible extended ribbon conformation in solution. Conformations of structural elements shared by each PS are indistinguishable. Differences in conformations are minor and localised at the sites of structural variations; there is no evidence of long-range stabilisation of a secondary structure. It is likely that antigenic specificity of Group 9 PS is dominated by local structural variation rather than by conformational differences.

Keywords: Conformation; ^{1}H NMR; ^{13}C NMR; Simulated annealing; Molecular dynamics. *Streptococcus pneumoniæ*

1. Introduction

S. pneumoniæ serogroup 9 comprises four structurally-distinct capsular polysaccharide (CPS) types (Types 9N, 9L, 9A, and 9V), two of which (9N and 9V) are used in pneumococcal vaccine formulations. Each Group 9 PS is a high molecular-weight ($\sim 10^6$

[1] Also at Birkbeck College, University of London. Current address:Biochemistry Department, University of Dundee, Dundee DD1 4HN, United Kingdom.

SSDI 0008-6215(94)00212-X

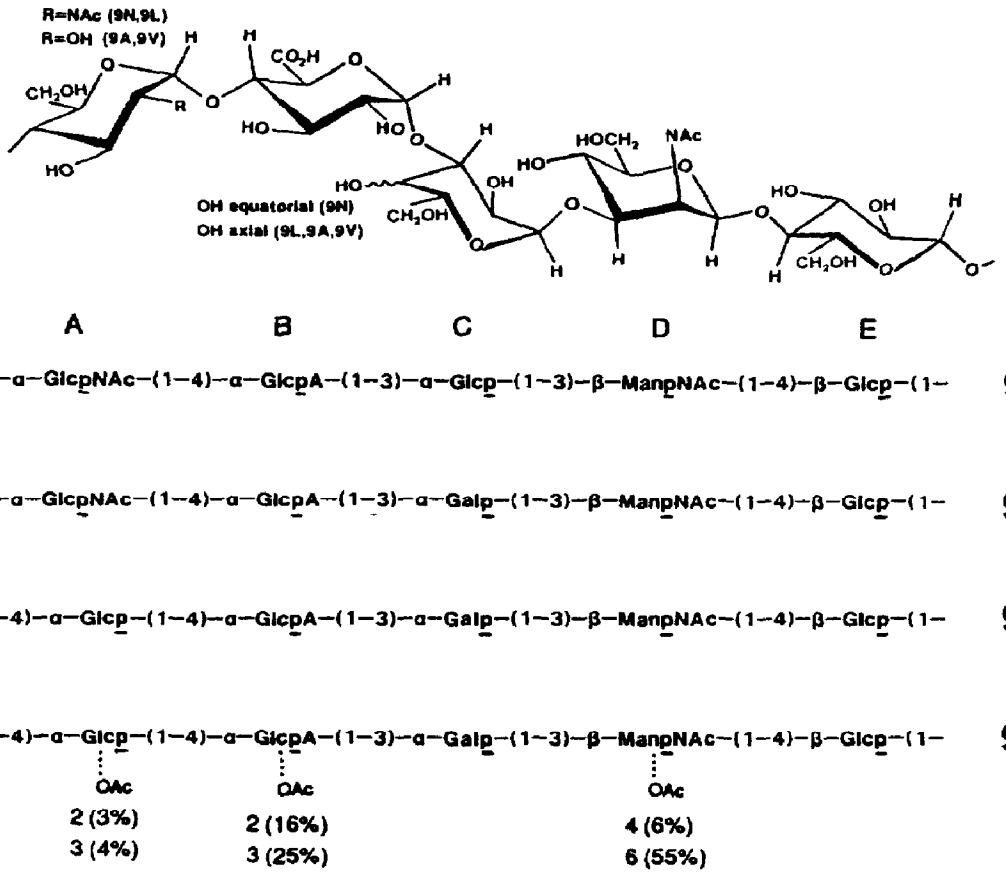

Fig. 1. Structures of the repeating units of capsules assigned to Serogroup 9.

Da) polymer with a linear pentasaccharide repeating unit (Fig. 1). Residues are labelled A–E for convenient specification of atom numbering. The structures of Types 9N [1] (S9 in American nomenclature) and 9L [2] (S49) differ only in the configuration of C-4 in residue C (Glc in 9N, Gal in 9L); 9A [3] (S33) differs from 9L only by a single NAc vs. OH substitution on residue A (GlcNAc in 9L, Glc in 9A); 9V [4] (S68) is an *O*-acetylated 9A sequence, with a complex pattern of *O*-acylation [5]. For the PS series studied in this work (9N, 9L, 9A) it can be seen from the structures summarised in Fig. 1 that residues B, D, and E are conserved, with changes occuring in residue A (Glc vs. GlcNAc) and residue C (Glc vs. Gal).

Despite close structural similarity, only partial antigenic cross reactivity between each Group 9 PS has been documented [6]. We have investigated the aqueous solution conformations of the Group 9 capsules in order to increase our understanding of the basis of antigenic molecular recognition. Methods for the conformational searching of carbohydrates have been reviewed [7]: in brief, hexapyranoside rings are considered approximately rigid and the conformation of the polymer depends on the relative orientation of adjacent residues; i.e., upon the glycosidic dihedral angles ϕ(H-1′–C-1′–O-α–C-α) and ψ(C-1′–O-α–C-α–H-α). The experimental problem is to determine sufficient interresidue constraints to define these angles.

There are relatively few reports based on experimental data for solution conformations of heteropolysaccharides, but we have determined the solution conformation of the Type 9N PS using a combination of NMR data and molecular modelling calculations [8]. Here we report a similar conformational analysis of PS Types 9L and 9A for comparison. The Type 9V PS has a heterogeneous *O*-acetylation pattern [5] and the complexity of its NMR spectra precludes this form of conformational analysis.

2. Experimental

NMR spectroscopy.—Prior to NMR studies, the exchangeable protons of the sample were deuteriated by lyophilisation from D_2O and dissolved in D_2O (Goss Scientific Instruments Ltd., Ingatestone, UK; 0.5 mL nominally 100%). 500-MHz ^1H NMR spectra were measured using a Jeol GSX-500 spectrometer. Spectral windows were chosen to include all signals of interest, generally 3.0–5.6 ppm. ^{13}C NMR spectra (67.5 MHz) were recorded on a Jeol GSX-270 spectrometer. All experiments used standard pulse programs with a nominal probe temperature of 70°C.

NOESY spectra were acquired in phase-sensitive mode using the complex transform procedure of States et al. [9]. One-dimensional truncated driven NOE experiments were performed using the Jeol microprogram NOEPUL, alternately acquiring on-resonance and subtracting off-resonance transients. A recycle time of 5 s (ca. $5 \times T_1$) was allowed for relaxation between each pulse. The optimum preirradiation time (300 ms) was determined from time-course experiments.

Chemical shifts were measured relative to that of internal 3-(trimethylsilyl)propionate-2,2,3,3-d_4 (sodium salt, Aldrich) at 0 ppm for ^1H and -1.8 ppm for ^{13}C resonances.

Molecular modelling.—Computer models were built using the Insight molecular modelling package (version 2.8, Biosym Technologies, San Diego, CA) running an Iris Indigo computer. Energy calculations used the AMBER force field [10] with the carbohydrate parameter set described by Homans [11]. Simulated annealing with NOE constraints was performed in vacuo, with a dielectric constant $\varepsilon = 80$ to part simulate bulk water. All torsion terms were scaled by a factor of 5 and molecular dynamics (MD) calculations were made at 500, 450, 400, and 350 K. Torsion terms were rescaled and the temperature was reduced from 300 to 0 K in 10 K steps, running 1 ps of MD at each temperature. The annealed structure was used as the input to a restrained md simulation (i.e., with NOE constraints), which was also run in vacuo ($\varepsilon = 80$). The MD history was recorded after every 250 steps of 1 fs.

3. Results and discussion

Glycosylation shifts.—Resonance assignments for the polysaccharides were required both for interpretation of NOE experiments and for calculation of glycosylation shifts. Glycosylation shifts (i.e., the difference in chemical shift of a resonance in the polymer compared with the corresponding resonance in the free monosaccharide) depend in part upon conformation and have long been used as qualitative evidence for close proximity of pendant

Table 1
^{1}H Chemical shifts (ppm) for Group 9 polysaccharides at 70°C [a]

	Residue	H-1	H-2	H-3	H-4	H-5	H-6	H-6′
A	9N	5.38	**3.91**	3.83	3.68	3.91	3.81	3.76
	9L	5.38	**3.92**	3.82	3.68	3.92	[b]	[b]
	9A	5.42	**3.54**	3.79	3.59	3.86	[b]	[b]
B	9N	5.33	3.61	3.92	3.75	4.32		
	9L	5.09	3.64	3.97	3.77	4.28		
	9A	5.09	3.66	4.03	3.78	4.25		
C	9N	5.24	3.61	3.75	**3.61**	3.79	3.91	3.82
	9L	5.31	3.95	3.82	**4.18**	4.13	3.76	3.76
	9A	5.30	3.95	3.83	**4.18**	4.13	3.76	3.76
D	9N	4.86	4.61	3.91	3.76	3.46	3.91	3.79
	9L	4.87	4.61	3.95	3.75	3.46	3.92	3.81
	9A	4.87	4.61	3.94	3.75	3.47	3.91	3.80
E	9N	4.49	3.35	3.64	3.64	3.53	3.84	3.65
	9L	4.50	3.35	3.65	3.65	3.53	3.85	3.70
	9A	4.47	3.35	3.64	3.64	3.52	3.84	3.69

[a] Data for the sites of structural variation are shown in bold face.
[b] Not assigned, being in a crowded region between 3.5–4.0 ppm.

groups in oligosaccharides [12]. ^{1}H and ^{13}C NMR resonances of the Type 9L PS were assigned from ^{1}H–^{1}H COSY, relayed-COSY, and ^{13}C–^{1}H HETCOR experiments using analogous reasoning to that previously reported for Types 9N [8] and 9A [5]. ^{1}H and ^{13}C chemical shifts of each PS are listed in Tables 1 and 3, respectively, and glycosylation shifts are shown in Tables 2 and 4, respectively. Raw NMR data and full details of the resonance assignments are given elsewhere (T.J. Rutherford, Ph.D. Thesis, University of London, 1991). Chemical shifts of monosaccharides in D_2O solution at 70°C were taken from the work of Jansson et al. [13].

An important feature to recognise from the chemical shift assignments is that the minor structural differences between these PS cause highly localised differences in glycosylation shifts, which are not transmitted far along the chain. Types 9L and 9A have similar shifts for all resonances, with all differences <0.04 ppm except for H-2(A), H-5(A), and H-3(B), which are all close in the sequence to the site of the structural variation (hydroxyl vs. acetamide on C-2(A)). Types 9N and 9L show larger glycosylation shift differences in residue C and for H-1(B), H-3(B), and H-3(D); all of these signals are from atoms close to the site of the structural variation, the configuration of C-4(C). There is also 0.05 ppm difference for H-$6_{pro\text{-}S}$(E) in 9L compared with 9N.

Most ^{1}H glycosylation shifts are positive; the only negative shifts are for H-5(C) and H-5(D) of 9N and some anomeric and hydroxymethyl signals. The β-anomeric protons in each PS (residues D and E), and the α-anomeric proton H-1(B) in 9L and 9A, have large negative glycosylation shifts (-0.14 to -0.17 ppm) indicating that the closest interresidue contacts are with protons rather than oxygens [14]. Positive shifts for all other H-1 resonances indicate proximity of these protons with oxygen atoms. Significant shifts for H-6(C) and H-6(E) protons reveal their likely involvement in interresidue interactions.

In ^{13}C spectra Types 9L and 9A have remarkably similar shifts for all resonances except C-2(A), the site of structural variation, and C-4(B), the linkage position on the adjacent

Table 2
^{1}H Glycosylation shifts (ppm) for each Group 9 capsular polysaccharidea [a]

	Residue	H-1	H-2	H-3	H-4	H-5	H-6	H-6′
A	9N	+0.17	**+0.03**	+0.06	+0.17	+0.03	−0.04	−0.01
(4-linked)	9L	+0.17	**+0.04**	+0.07	+0.19	+0.06	[b]	[b]
	9A	+0.19	**0.00**	+0.07	+0.17	+0.02	[b]	[b]
B	9N	+0.07	+0.02	+0.15	+0.20	+0.21		
(4-linked)	9L	−0.15	+0.07	+0.22	+0.24	+0.19		
	9A	−0.15	+0.09	+0.28	+0.25	+0.16		
C	9N	+0.01	+0.05	+0.01	**+0.17**	−0.07	+0.07	+0.06
(3-linked)	9L	+0.09	+0.17	+0.01	**+0.23**	+0.10	+0.07	+0.07
	9A	+0.08	+0.17	+0.02	**+0.23**	+0.08	+0.07	+0.07
D	9N	−0.17	+0.14	+0.06	+0.22	−0.01	−0.01	−0.04
(3-linked)	9L	−0.14	+0.16	+0.12	+0.22	+0.01	+0.02	0.00
	9A	−0.14	+0.16	+0.11	+0.22	+0.02	+0.01	0.00
E	9N	−0.17	+0.08	+0.12	+0.20	+0.05	−0.06	−0.07
(4-1inked)	9L	−0.14	+0.10	+0.15	+0.23	+0.07	−0.05	−0.02
	9A	−0.17	+0.10	+0.14	+0.22	+0.06	−0.06	−0.03

[a] Protons on linkage carbons are underlined. Data for the sites of structural variation are shown in bold face.
[b] Not assigned in the polysaccharide.

Table 3
^{13}C Chemical shifts (ppm) of Types 9N, 9L, and 9A polysaccharides at 70°C (and chemical shift changes, in ppm, between 25 and 70°C) [a]

	Residue	C-1	C-2	C-3	C-4	C-5
A	9N	97.5 (−0.07)	**54.3 (0.02)**	70.4 (0.15)	79.7 (0.49)	71.6 (0.05)
	9L	97.7 (−0.08)	**54.4 (0.04)**	70.4 (0.13)	79.8 (0.51)	71.7 (0.08)
	9A	99.0 (−0.06)	**72.5 (0.16)**	72.5 (0.16)	79.4 (0.59)	71.5 (0.03)
B	9N	99.9 (0.03)	71.3 (0.05)	74.4 (−0.26)	77.4 (0.47)	73.8 (0.21)
	9L	95.8 (0.35)	72.5 (−0.01)	74.5 (−0.20)	77.6 (0.52)	73.8 (0.19)
	9A	95.7 (0.23)	72.1 ([b])	74.2 (−0.27)	78.6 (0.91)	73.6 (0.08)
C	9N	101.6 (−0.02)	72.9 (0.00)	80.8 (0.80)	**71.0 (−0.08)**	73.1 (0.03)
	9L	101.2 (0.26)	67.9 (0.11)	75.2 (0.57)	**66.7 (0.27)**	72.1 (−0.24)
	9A	101.2 (0.25)	67.8 (0.04)	74.9 (0.43)	**66.6 (0.22)**	72.1 (−0.22)
D	9N	100.2 (−0.10)	53.7 (−0.13)	79.3 (0.31)	67.6 (0.13)	77.2 (−0.03)
	9L	100.3 (−0.07)	53.7 (−0.07)	78.2 (0.79)	67.8 (0.11)	77.4 (−0.06)
	9A	100.3 (−0.12)	53.6 (−0.19)	78.2 (0.76)	67.8 (0.04)	77.3 (−0.11)
E	9N	103.3 (−0.05)	74.0 (0.08)	74.9 (0.18)	79.6 (−0.05)	75.5 (0.07)
	9L	103.4 (−0.06)	74.1 (0.11)	75.0 (0.23)	79.7 (−0.04)	75.6 (0.06)
	9A	103.4 (−0.05)	74.0 (0.05)	74.9 (0.13)	79 7 (−0.11)	75.6 (0.06)

[a] Hydroxymethyl C-6 resonances: 9N 61.4, 61.3, 61.1, and 60.7 ppm; 9L 62.4, 61.5, 61.3, and 60.8 ppm; 9A 62.5, 62.3, 61.2, and 60.8 ppm were not assigned to individual carbon atoms. Data for the sites of structural variation are shown in bold face.
[b] Not resolved.

Table 4
^{13}C Glycosylation shifts (ppm) for Group 9 polysaccharides at 70°C [a]

	Residue	C-1	C-2	C-3	C-4	C-5
A	9N	+5.7	**−0.7**	−1.3	+8.4	−0.9
(4-linked)	9L	+5.9	**−0.6**	−1.3	+8.5	−0.8
	9A	+6.0	**0.0**	−1.3	+8.7	−0.9
B	9N	+6.9	−1.0	+0.9	+4.5	+1.3
(4-linked)	9L	+2.8	+0.2	+1.0	+4.7	+1.3
	9A	+2.7	−0.2	+0.7	+5.7	+1.1
C	9N	+8.6	+0.4	+7.0	**+0.2**	+0.7
(3-linked)	9L	+8.0	−1.5	+5.1	**−3.6**	+0.8
	9A	+8.0	−1.6	+4.8	**−3.7**	+0.8
D	9N	+6.3	−1.2	+6.3	0.0	0.0
(3-linked)	9L	+6.4	−1.2	+5.2	+0.2	+0.1
	9A	+6.4	−1.3	+5.2	+0.2	+0.1
E	9N	+6.5	−1.2	−1.9	+8.9	−1.2
(4-linked)	9L	+6.6	−1.1	−1.8	+9.0	−1.2
	9A	+6.6	−1.2	−1.9	+9.0	−1.2

[a] Data for the sites of structural variation are shown in bold face.

residue. Type 9L has seven glycosylation shifts that differ from those of 9N by 0.5 ppm or more [C-1(B), C-2(B), C-1 through C-4 in residue C and C-3(D)], each of which is close to the epimerised C-4(C). The similarity of shifts for all other residues indicates that any conformational differences between these polymers occur only at linkages adjacent to the sites of structural variation.

A satisfactory molecular model must show evidence of interactions that would cause the observed significant conformation-dependent chemical shifts. The overall patterns of ^{13}C glycosylation shifts of resonances for linkage carbon ('α-carbon') and the adjacent carbons ('β-carbon') were consistent with the patterns observed by Shashkov et al. [15] for disaccharides, which have been explained in terms of stereochemical relationships. As might be expected from inductive effects alone, all α-carbon resonances have large (>2.5 ppm) downfield glycosylation shifts and these are the only resonances with absolute values >4 ppm. For a β-carbon with none of its pendant groups in proximity with neighbouring residues (i.e., exhibiting no conformation dependent effects) an up field shift (ca. 1.5 ppm) is expected [14,15]. Downfield shifts or large ($> \sim 2$ ppm) upfield shifts of β-carbon resonances indicate some conformational dependence [14,16] and are useful for structure prediction. The β-carbon shifts in this work which show significant (≥ 1 ppm) conformational dependence are C-2(A) (all PS), C-2(B) (9A, 9L), C-3(B) (all PS), C-5(B) (all PS), C-2(C) (9N), C-4(C) (9N), and C-4(D) (all PS).

Variable temperature effects on chemical shifts.—It was shown previously that ^{1}H chemical shifts for the Type 9N PS were insensitive to temperature [8], but ^{13}C chemical shifts may vary by up to 0.9 ppm between 25 and 70°C (Table 3). Chemical shifts are sensitive to changes in the 'virtual' (time-averaged) conformation of polysaccharides, and if the PS occupies either a single assymetric conformational energy well or a series of different energy wells, the 'virtual' conformation will be temperature dependent. Temperature sensitive

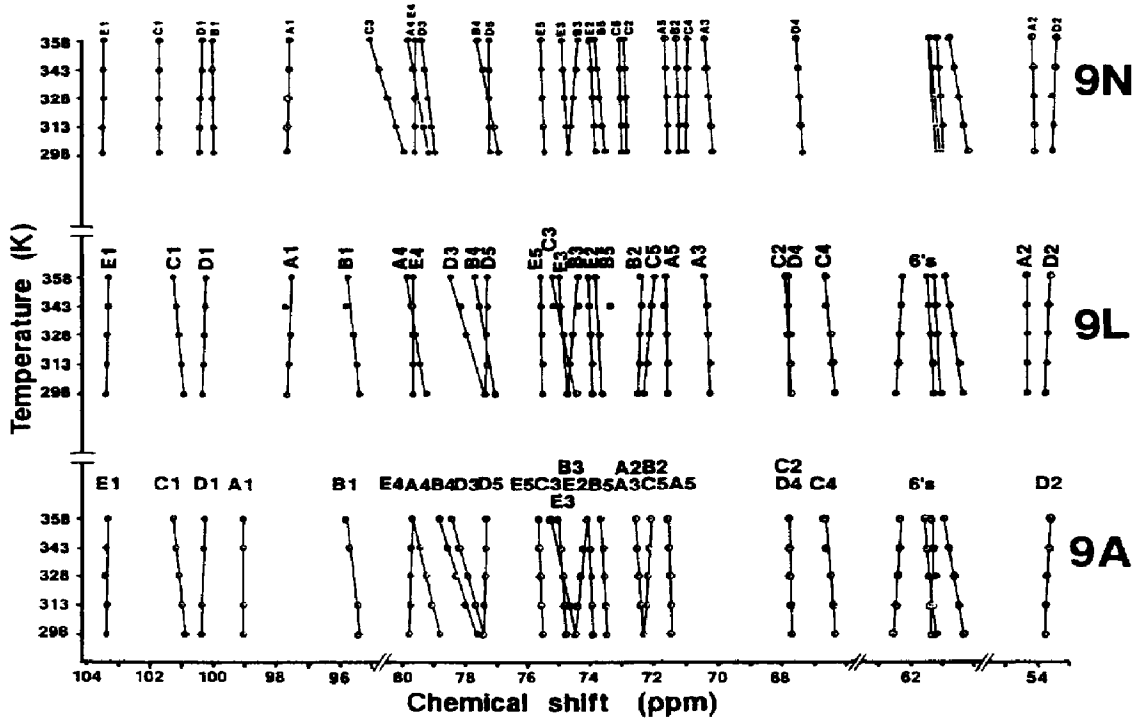

Fig. 2. Temperature vs. ^{13}C chemical shifts for PS Types 9N, 9L, and 9A.

shifts should indicate which nuclei are involved in interresidue steric interactions that change with temperature.

The ^{13}C temperature dependence of each Group 9 PS is shown in Fig. 2. Most resonances showed small, approximately linear, reversible shift variations over this temperature range, although the direction of the slope ($\Delta\delta/\Delta T$) varied. C-1 resonances show small negative slopes for (1→4)-linkages and small positive slopes for (1→3)-linkages. Comparison of slopes for the different polysaccharides showed significant differences only for resonances that are close to the sites of structural variation. Some interesting small differences in the temperature dependence of shifts occur in the conserved residues, B and D, which must result from structural changes in adjacent residues. These differences are largest for the linkage carbons C-1(B) and C-3(D), where 9L = 9A ≠ 9N and C-4(B) where 9N = 9L ≠ 9A.

Conformation-dependent shifts are difficult to interpret quantitatively, since they are affected by the interatomic distances, angles of approach, and orientation of any lone-pairs between each interacting pendant group in the molecules, which exhibit internal flexibility (as indicated by the relatively narrow NMR linewidths for these high-MW polymers). However, Bock et al. [17] derived a calibration curve relating C-1′ and C-α chemical shifts with the glycosidic dihedral angle, ψ. According to this curve, a change of 10° in the time-averaged ψ angle causes a 1–2 ppm change in the aglycon C-α chemical shift. The largest C-α chemical shift changes for the Group 9 PS between 25 and 70° C is 0.9 ppm, indicating a 0–5° change in ψ which is well within the error limits of determining conformations from NOE measurements. Hence the overall conformational equilibria at 25°C are similar to

those at 70° C. Changes in ψ should also be reflected in the C-1 chemical shift, although these were considerably less temperature-sensitive than C-α shifts.

In summary, the conformation-dependent chemical shift parameters for the three PS are virtually identical for residues D (except for the linkage position) and E. The structural differences result in conformational changes that are restricted to linkages A–B (for the GlcNAc vs. Glc substitution) and B–C and, possibly, C–D (for the Glc vs. Gal epimerisation).

NOE experiments.—All interresidue correlations in Group 9 PS NOESY spectra (not shown) were between sequentially-adjacent residues and involved either anomeric protons or equatorial protons adjacent to the linkage positions. There were no 'long-range' correlations that might indicate a tightly-coiled secondary structure, which is consistent with the extended ribbon conformation proposed for Type 9N [8]. Enhancements were quantified from optimised one-dimensional truncated-driven difference experiments, irradiating each anomeric proton and β-ManNAc H-2 [H-2(D)] separately. With a preirradiation time of 300 ms, the initial rate approximation applies to the observed enhancements, for which the NOE is directly proportional to r^{-6} (for an isotropically tumbling rigid rotor). The results are presented in Table 5 in the form of relative NOEs; i.e., expressed as a ratio of the magnitude to a reference NOE. The shortest intraresidue ^{1}H–^{1}H distance from the presaturated nucleus was taken for NOE reference values (H-1···H-2 in α-sugars and H-1···H-5 in β-sugars).

Internuclear distance calculations.—A simple ratio calculation was used to estimate interresidue ^{1}H–^{1}H distances. Reference distances were obtained from MM2CARB optimised monosaccharide models (H-1···H-2 = 0.248 nm, H-1···H-5 = 0.250 nm for β-ManNAc and 0.237 nm for β-Glc). Using the NOE-ratio approach assumes that each ^{1}H–^{1}H vector has approximately the same rotational correlation time, τ_c. From ^{13}C T_1 data for both 9N and 9A [mean T_1 256 ms (SD 47) for 9N and 282 ms (SD 58) for 9A], it was concluded that the most suitable motional model is that of an isotropic rotor with $\tau_c \sim 5$ ns (assuming dipole–dipole relaxation with the directly attached proton as the sole relaxation mechanism).

Interresidue ^{1}H–^{1}H distances calculated for each PS are shown in Table 5. It is generally accepted that error limits of NOE measurements are $\pm$ 10–20%, and the corresponding error limits on the estimated ^{1}H–^{1}H distance is, therefore, $\pm$ 0.01 nm. In practice there is a greater uncertainty in the interresidue ^{1}H–^{1}H distance estimates, resulting from attenuation of the NOE by the effects of internal motions [18]. Modelling constraints were applied with wide error limits ($\pm$ 20% of the distance) to allow for uncertainties in the experimentally-derived distance estimates. A 20% change in distance corresponds approximately to a three-fold change in measured NOE

Due to almost complete overlap of H-3(E), H-4(E), and H-4(A) peaks for 9N and 9L it was not possible to measure a H-1(E)···H-4(A) NOE directly. The NOE ratio for H-1(E)···H-4(A) in Table 5 also includes the H-1(E)···H-3(E) NOE The interresidue H-1(E)···H-4(A) distance was estimated after subtracting the estimated contribution from H-1(E)···H-3(E). NOE enhancements were observed between H-2(D) and H-5(C), but the spectra were difficult to phase correctly since the irradiated resonance, H-2(D), is close to the residual water peak. Hence the H-2(D)···H-5(C) NOE was not quantified accurately, but rough estimates of ^{1}H–^{1}H distances were made to provide a distance constraint for modelling studies.

Table 5
Experimental relative NOE ratios, distance constraints (nm) for MD simulations (r_{min}, r_{max}) and Tropp-averaged ^1H–^1H distances calculated from models

Link	9N σ_{ref}/σ	$r_{min}-r_{max}$	r_{Tropp}	r_{exptl} [a]	9L σ_{ref}/σ	$r_{min}-r_{max}$	r_{Tropp}	r_{exptl} [a]	9A σ_{ref}/σ	$r_{min}-r_{max}$	r_{Tropp}	r_{exptl} [a]
H-1(A)···H-3(B)	2.98	0.23–0.35	0.269	0.29	1.70	0.22–0.32	0.266	0.27	1.39	0.21–0.31	0.287	0.26
H-1(A)···H-3(B)	[b]	0.26–0.38	0.376	[b]	4.25	0.26–0.38	0.375	0.32		0.30–0.99	0.418	>0.3
H-1(B)···H-3(C)	1.94	0.22–0.34	0.265	0.28	2.77	0.24–0.36	0.288	0.30	3.93	0.25–0.36	0.321	0.25
H-1(B)···H-4(C)	[b]		0.395	[b]	1.10	0.20–0.30	0.258	0.25	0.99	0.29–0.30	0.267	0.25
H-1(C)···H-3(D)	1.06	0.20–0.30	0.256	0.25	[b]	0.20–0.30	0.25	[b]	[b]	0.20–0.30	0.266	[b]
H-2(D)···H-5(C)	[c]	0.21–0.31	0.261	0.26 [c]	[c]	0.22–0.34	0.268	0.28 [c]	[c]	0.22–0.34	0.289	0.28 [c]
H-1(D)···H-4(E)	0.37	0.18–0.24	0.248	0.20	0.68	0.18–0.26	0.253	0.22	0.66	0.18–0.26	0.270	0.22
H-1(E)···H-4(A)	0.91	0.18–0.30	0.269	0.25	0.92	0.18–0.28	0.274	0.23	1.36	0.18–0.30	0.285	0.25
H-1(E)···H-6(A)	2.05	0.25–0.36	0.329	0.31	2.12	0.23–0.35	0.300	0.29	9.39	0.27–0.41	0.393	0.34

[a] Distance calculated from experimental data.
[b] Obscured by peak overlap.
[c] Overestimated.

The major feature to recognise is that, once again, there are relatively small differences in the experimentally-derived parameters for each of these polymers, hence each has a similar conformation. Differences in the data for each polymer occur across linkages to the nonconserved residues and are within the error limits of the measurements for the structural elements shared by two or more polymers. As with glycosylation shifts, the patterns and relative magnitudes of measured NOE for the polymers were consistent with previous reports for disaccharides [19]; hence the conformation of the polymer is a summation of the conformations of individual disaccharide elements, with no evidence of contributions resulting from a more stable polymer secondary structure.

Molecular modelling calculations.—Models of the nonasaccharide (the pentasaccharide repeating unit plus two residues on each end to account for 'end effects') of each PS structure were energy minimised by simulated annealing with NOE constraints (Table 5), as described for 9N in Ref. [8]. Minimizing the structures in the presence of experimentally-derived constraints reduces the dependence of the energy calculations on assumptions about the force field, the effects of hydration, and the contribution of factors such as the exo-anomeric effect. Models depicting the annealed structures are shown in Fig. 3.

510 ps of restrained molecular dynamics (MD) were run for each annealed nonasaccharide model in vacuo. The ϕ,ψ trajectories during the simulation are shown in Fig. 4. The first 10 ps of the simulation were regarded as an equilibration period and were discarded before back-calculating NMR effective ^{1}H–^{1}H distances (Table 5). Effective distances were calculated using the Tropp formalism [20] to account for multi-site conformational exchange that is rapid compared with molecular rotational correlation times. Homans and Forster have demonstrated the suitability of the Tropp formalism for conformational averaging in small oligosaccharides [21]. The Tropp-averaged distances in Table 5 are in close agreement (± 0.02 nm) with experimentally-derived ^{1}H–^{1}H distance estimates. The largest observed differences between theoretical and experimental distances are ca. 0.05 nm for H-1(A)···H-3(B) (9N and 9L), H-1(D)···H-4(E) (each PS), H-1(E)···H-4(A) (9L and 9A), and H-1(E)···H-6(A) (9A), which is still satisfactory agreement.

The models were examined for any short time-averaged ^{1}H–^{1}H distances (<0.35 nm) that were not evident from the NOE experiments. For each group 9 PS model the effective time-averaged (r_{Tropp}) distance between H-5(B) and H-3(C) was 0.30–0.33 nm, which should give rise to a small observable NOE. For Type 9N this NOE would be obscured by overlap of H-3(C) and H-4(B) resonances, although this low intensity correlation was not observed in NOESY spectra of Types 9L or 9A. The only other short ^{1}H–^{1}H distances that occurred in the models but were not evident from NOE experiments were for the two β-(1→4)-linkages (D–E and E–A); H-1 of the glycoside to H-6 protons on the aglycon. The simulated distances (the shortest being 0.29 nm) were sensitive to the orientation of the hydroxymethyl group. For example, for the two E–A linkages in the 9A nonasaccharide model the H1(E)···H6S(A) distance was 0.29 and 0.41 nm, although the glycosidic dihedral angles agreed to within $\pm 0.6°$. Clearly, 500 ps of MD simulation is insufficient to reproduce motions on the timescale of hydroxymethyl group rotations, and it is not surprising that NOEs are not observed to H-6 spins when the models imply enhancements that are close to the limit of detection.

Glycosylation shifts for 9N were previously rationalised in terms of steric proximity in MD simulations [8]. Similarly the ^{13}C conformation-dependent shifts for 9L and 9A can

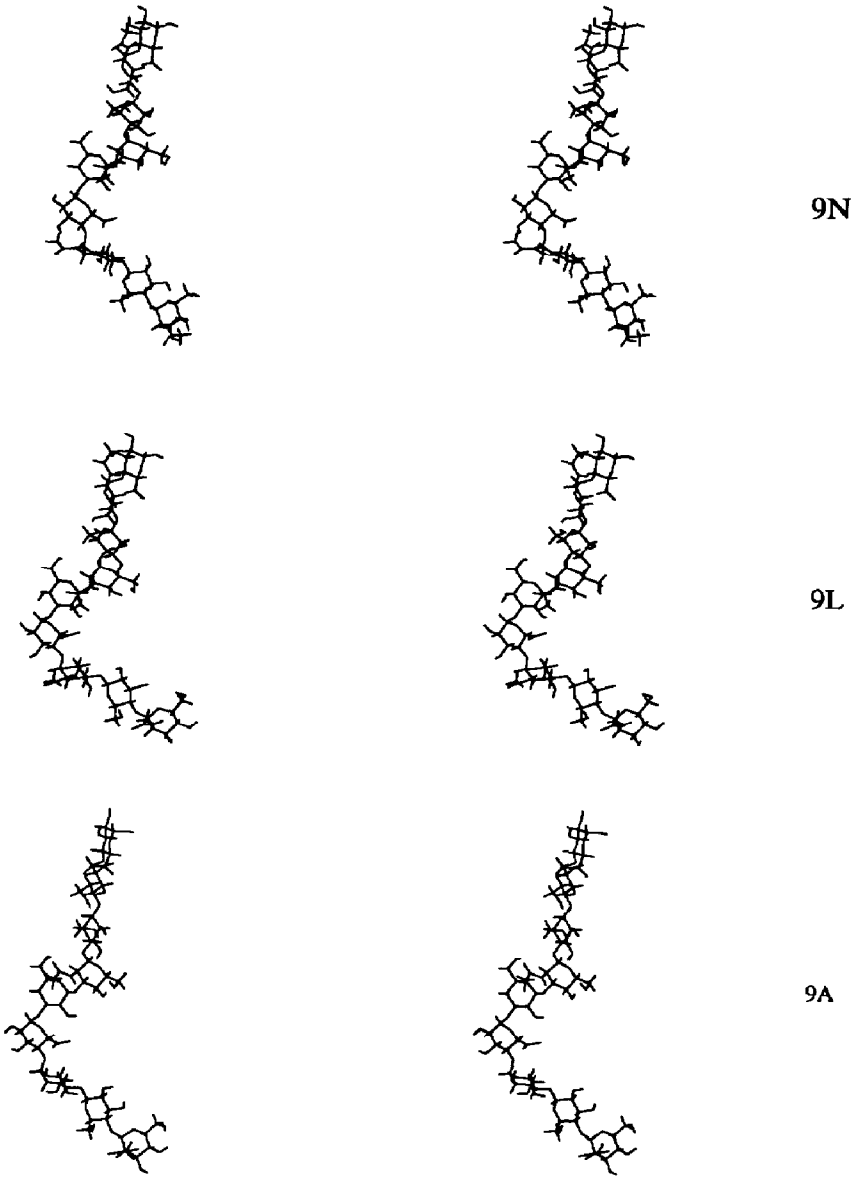

Fig. 3. Stereo images of annealed nonasaccharide models of Group 9 PS fragments.

be explained by the close proximity (<0.35 nm time-averaged distance) of the carbon's pendant groups with neighbouring saccharide rings. C-3(B) is shifted by the close approach of H-1(A) and O-3(B), H-5(B)···O-2(C) proximity affects both attached carbon shifts (although to a lesser extent for C-2(C) in 9L and 9A), the H-5(C)···H-2(D) proximity (as noted in NOE experiments) influences C-5(C) and, H-1(C)···H-4(D) influences C-4(D). The glycosylation shift of C-4(C) is positive for 9N, where its attached oxygen is close to H-1(B), but negative in the *galacto* configuration (9L and 9A), where its attached proton is presented to H-1(B). The reason for the large difference in C-2(B) glycosylation shifts in 9N and 9L is less clear, but it might result from occasional hydrogen bond formation

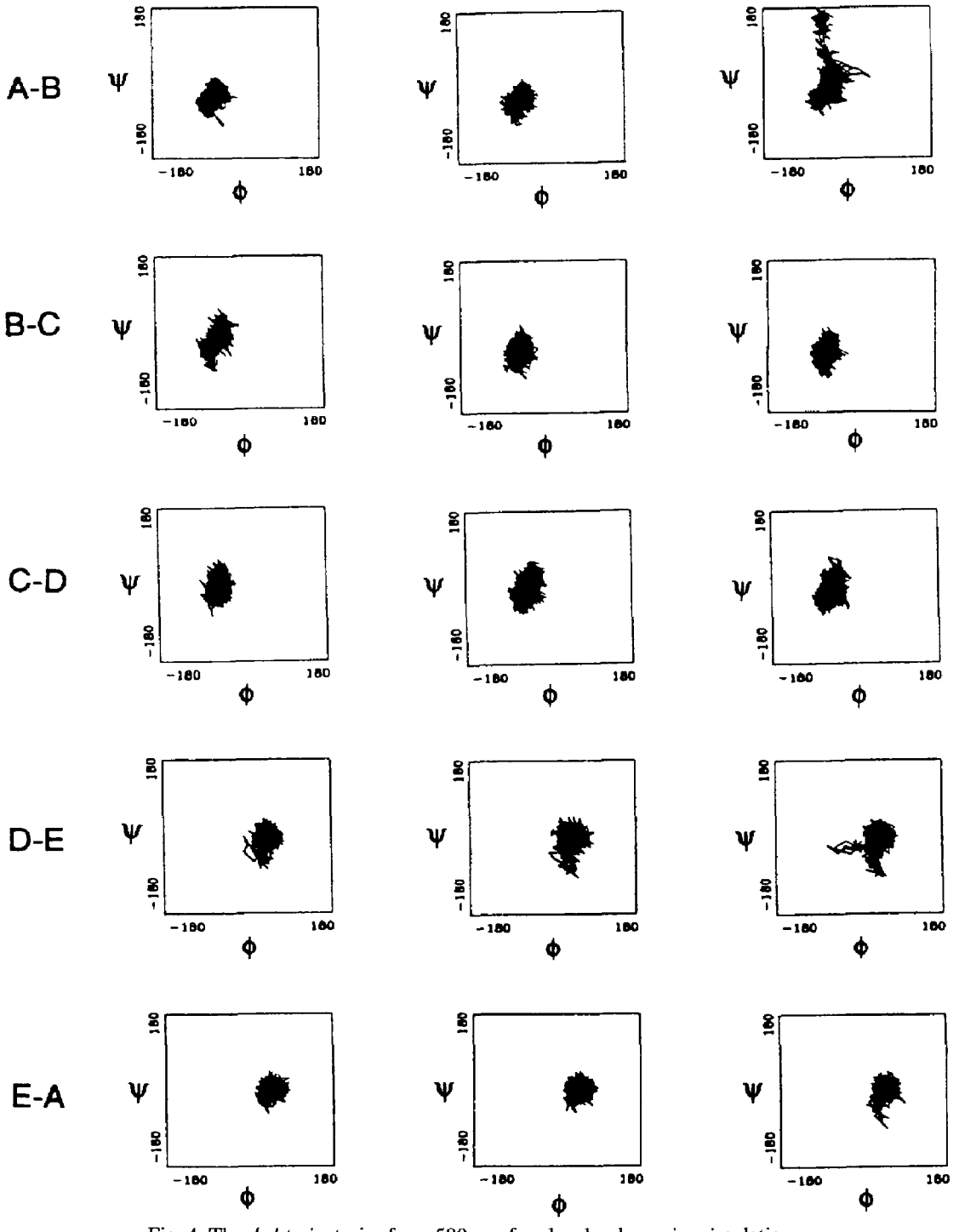

Fig. 4. The ϕ,ψ trajectories from 500 ps of molecular dynamics simulations.

between O-2(B) and the Gal/Glc O-4 ($<r>$ =0.4 nm during the dynamics run).

The simple time-averaged ϕ and ψ torsion angles for each model (Table 6) show that each PS exhibits a conformational equilibrium which is centred at similar positions on the

Table 6
Time-averaged ϕ; ψ torsion angles (rms deviation) from 500 ps MD simulations

Link	9N	9L	9A
A–B	−44 (11); −25 (15)	−43 (10); −24 (14)	−42 (13); −6 (41)
B–C	−50 (11); −16 (20)	−53 (9); −34 (17)	−55 (9); −36 (17)
C–D	−51 (7); −3 (18)	−50 (9); −3 (20)	−50 (9); −3 (19)
D–E	45 (13); −3 (15)	46 (15); −1 (17)	46 (16); −2 (19)
E–A	49 (13); 0 (12)	49 (13); 1 (13)	50 (13); 2 (14)

ϕ,ψ surfaces. Both of the structural changes in these three PS models cause a single change of $\sim 20°$ in a time-averaged ψ torsion angle. The modelling calculations give an overall picture of the likely conformational equilibrium, but are not sensitive enough to distinguish other small differences for these polymers that may be indicated by the minor variations in NMR parameters.

Characteristics of the models and implications for biological activity.—The helical rise of the annealed models, measured between two C-1(B) atoms, is 2.24 ± 0.02 nm. This value is 95% of the maximum possible extension and is comparable with observations of a variety of plant and animal polyuronides in the solid state (82–96%) [22]. The maximum size of an antibody binding site is ~ 3 nm [23,24], which approximates to 6–7 sugar residues or 1.5 repeating units.

Szu et al. [6] established that the carboxylate functional group on residue B is an essential requirement for recognition of the Group 9 antigen. It has also been suggested that *O*-acetyl groups are immunodominant features in carbohydrate epitopes [25], and it is likely that *N*-acetyl groups have a similar immunological rôle. In models of the most favoured solution conformations of Group 9 PS, two conserved functional groups, the uronic acid carboxylate (residue B) and the ManNAc *N*-acetyl (residue D), are in close spatial proximity (< 0.6 nm time averaged) on one side of the extended chain. The sites of structural variation (and each of the sites that are *O*-acetylated on the 9V PS) are on the opposite face of the chain to the conserved groups. Hence, we propose a mechanism by which antibodies can recognise a Group 9 epitope that is conserved in each PS (in part from residues B and D), yet other antibodies directed towards the opposite face (mainly in residues A and C) can distinguish between each member of the group.

Studies of the PS from *Neisseria meningitidis* Groups B and C showed that anti-capsular antibodies can be directed towards either conformational or sequential epitopes [26]. For conformational epitopes, no binding is observed for polymer fragments shorter than ~ 10 residues, since shorter fragments cannot adopt the required conformational motif. However, sequential binding sites are inhibited by fragments as small as di- or tri-saccharides [27]. It has been established that antibody binding to the *S. pneumoniæ* Type 9N PS is inhibited by disaccharide fragments [28]. By absorbing type-specific polyclonal antisera with a single heterologous PS and measuring the reactivity of each Group 9 PS with the residual antibodies, it was demonstrated that Type 9L shows strong cross-reactivity with all other types and has epitopes that are found on 9N but not 9A and 9V and other epitopes that are found on 9A and 9V but not 9N [6]. Types 9A and 9V do not react with anti-9N antibodies that are not absorbed by 9L. These observations are consistent with a recognition process involving a sequential epitope.

4. Conclusions

The PS Types 9N, 9L, and 9A, have very similar conformations in aqueous solution. NMR data and restrained MD simulations indicate only minor differences in the conformational equilibria for these polymers. Dynamic models were in agreement with measured NOE data, and conformation dependent ^{13}C chemical shifts were rationalized in terms of close proximity of groups on adjacent residues. Combining previous immunochemical evidence with the current physicochemical data, it seems likely that Group 9 capsules have sequential epitopes; i.e., that antigenic specificity for Group 9 PS is determined by local structural variation rather than by conformational differences.

Acknowledgements

We thank the S.E.R.C. for a CASE studentship (T.J.R.) and access to 500-MHz NMR facilities (Birkbeck College, U.L.I.R.S.), the M.R.C. Biomedical NMR Centre (Mill Hill) for access to NMR facilities, Merck, Sharpe, and Dohme for their gift of the Type 9N PS, and Steve Homans, Mark Forster, and Martin Kipps for helpful discussions.

References

[1] C. Jones, B. Mulloy, A. Wilson, A. Dell, and J.E. Oates, *J. Chem. Soc., Perkin Trans. 1*, (1985) 1665–1673.
[2] J.C. Richards, M.B. Perry, and P.J. Kniskern, *Can. J. Biochem.*, 62 (1984) 1309–1320.
[3] J.C. Richards and M.B. Perry, in A.M. Wu (Ed.), *The Molecular Immunology of Complex Carbohydrates*, Plenum, 1988, p 594.
[4] M.B. Perry, V. Daoust, and D.J. Carlo, *Can. J. Biochem.*, 59 (1981) 524–533.
[5] T.J. Rutherford, C. Jones, D.B. Davies, and A.C. Elliott, *Carbohydr. Res.*, 218 (1991) 175–184.
[6] S. Szu, C.-J. Lee, D. Carlo, and J. Henrichsen, *Infect. Immun.*, 31 (1981) 371–379.
[7] A.D. French and J.W. Brady (Eds.), *Computer Modelling of Carbohydrate Molecules, ACS Symp. Ser.*, 430 (1990).
[8] T.J. Rutherford, C. Jones, D.B. Davies, and A.C. Elliott, *Carbohydr. Res.*, 265 (1994) 79–96.
[9] D.J. States, R.A. Haberkorn, and D.J. Ruben, *J. Magn. Reson.*, 48 (1982) 286.
[10] U.C. Singh, P. Weiner, J. Caldwell, and P.A. Kollman, AMBER 3.0, University of California, San Francisco, 1986.
[11] S.W. Homans, *Biochemistry*, 29 (1990) 9110–9118.
[12] R.U. Lemieux and K. Bock, *Arch. Biochem. Biophys.*, 221 (1982) 125–134; H. Thogersen, R.U. Lemieux, K. Bock, and B. Meyer, *Can. J. Chem.*, 60 (1982) 44–57.
[13] P.E. Jansson, L. Kenne, and E. Schweda, *J. Chem. Soc., Perkin Trans. 1*, (1987) 377–383.
[14] H. Baumann, Ph.D. Thesis, *Univ. Stockholm Chem. Commun.*, 9 (1988).
[15] A.S. Shashkov, G.M. Lipkind, Y.A. Knirel, and N.K. Kochetkov, *Magn. Reson. Chem.*, 26 (1988) 735–747.
[16] N.K. Kochetkov, O.S. Chizhov, and A.S. Shashkov, *Carbohydr. Res.*, 133 (1984) 173–185.
[17] K. Bock, A. Brignole, and B.W. Sigurskjold, *J. Chem. Soc., Perkin Trans. 2*, (1986) 1711–1713.
[18] D. Genest, *Biopolymers*, 28 (1989) 1903–1911.
[19] G.M. Lipkind, A.S. Shashkov, S.S. Mamyan, and N.K. Kochetkov, *Carbohydr. Res.*, 181 (1988) 1–12.
[20] J. Tropp, *J. Chem. Phys.*, 72 (1980) 6035–6043.
[21] S.W. Homans and M.J. Forster, *Glycobiology*, 2 (1992) 143–151.
[22] E.D.T. Atkins in R. Berkeley, G. Gooday, and D. Elwood (Eds.), *Microbial Polysaccharides and Polysaccharases*, Academic, London, 1979, Chap. 5.

[23] E.A. Kabat, *J. Immunol.*, 84 (1960) 82–85.
[24] M.R. Lifely, C. Moreno, and J.C. Lindon, *Vaccine*, 5 (1987) 11–26.
[25] B. Jann and K. Jann, *Bacterial Capsules*, Springer Verlag, Berlin, 1990.
[26] F. Michon, J.R. Brisson, and H.J. Jennings, *Biochemistry*, 26 (1987) 8399–8405.
[27] H.J. Jennings, R. Roy, and F. Michon, *J. Immunol.*, 134 (1985) 2651.
[28] J.D. Higginbotham, A. Das, and M. Heidelberger, *Biochem. J.*, 126 (1972) 225–231.